

PAPER • OPEN ACCESS

## Synthesis and characterization of Cu-doped TiO<sub>2</sub> thin films produced by the inert gas condensation technique

To cite this article: H A Ahmed *et al* 2017 *J. Phys.: Conf. Ser.* **869** 012027

View the [article online](#) for updates and enhancements.

### Related content

- [Relationship Between Photocatalytic Activity and Structure of TiO<sub>2</sub> Thin Film](#)  
Wen-zhen Zhang, Tao Zhang, Wen Yin et al.
- [XRD and XANES study of some Cu-doped MnBi materials](#)  
Ashutosh Mishra and Harsha Patil
- [TiO<sub>2</sub> Thin Films Formed by Electron Cyclotron Resonance Plasma Oxidation of Ti Thin Films](#)  
Yoshio Abe and Takuya Fukuda



**IOP | ebooks™**

Bringing together innovative digital publishing with leading authors from the global scientific community.

Start exploring the collection—download the first chapter of every title for free.

# Synthesis and characterization of Cu-doped TiO<sub>2</sub> thin films produced by the inert gas condensation technique

H A Ahmed<sup>1</sup>, S I Abu-Eishah<sup>2,\*</sup>, A I Ayesh<sup>3</sup> and S T Mahmoud<sup>4</sup>

<sup>1</sup> Materials Science & Eng. Program, UAE University, Al-Ain, UAE

<sup>2</sup> Department of Chemical & Petroleum Eng., UAE University, Al-Ain, UAE

<sup>3</sup> Department of Mathematics, Statistics and Physics, Qatar University, Doha, Qatar

<sup>4</sup> Department of Physics, UAE University, Al-Ain, UAE

Email: s.abueishah@uaeu.ac.ae

**Abstract.** The bandgap of thin films Cu-doped TiO<sub>2</sub> nanoclusters prepared using the inert gas condensation (IGC) technique have been investigated at various Cu contents. The samples were characterized using XRD, SEM/EDS and UV-visible spectrophotometer. It was found that doping of TiO<sub>2</sub> thin film nanoclusters with Cu enhance its optical activity and shift it to the visible region; which makes it useful in photocatalytic applications.

## 1. Introduction

Nanostructured materials can be synthesized by the most widely inert gas condensation (IGC) technique, which can control the size, distribution and purity of the nanoparticles by using a thermal evaporation source, an electron beam evaporation device or a sputtering source in an inert gas atmosphere of argon or helium[1]. IGC can produce particles of well-defined grain size and with a narrow size distribution and can also have the capability to modify the nano-sized morphology, crystallinity, and particle size [2-4].

## 2. Materials and research methods

### 2.1 Materials Used

Argon gas (99.999% purity) was used along with a mass flow controller (MKS Instruments, Andover, MA1810, USA) in the range of 0–100 sccm. Ti (99.9% pure) and Cu-Ti alloys sputtering targets (with 1.6, 3.2, 4.8, 6.4, and 8 wt.% Cu) supplied by Testbourne Ltd. (USA) with 50.8 mm diameter x 6.35 mm thickness.

### 2.2 Preparation and Characterization of the Cu-TiO<sub>2</sub> thin films

An ultra-high vacuum (UHV) compatible system with a nanocluster source of magnetron plasma sputtering and inert gas aggregation condensation (Nanogen-50, Mantis Deposition Ltd., Oxfordshire, UK) was used to produce the Cu-Ti nanoclusters. The procedure followed for sputtering is the same as that published earlier [5] but with some variation in the parameters. The nanocluster-based thin film samples were characterized by using X-ray diffraction (Shimadzu 6100 X-ray Diffractometer with Ni and Cu-K $\alpha$  radiation ( $\lambda = 0.15406$  nm)), Scanning Electron Microscope (variable pressure Tescan VEGA XM SEM) Energy Dispersive Spectrometer (EDS) (Oxford Instruments X-Max 50 EDS detector (LN2 free system) with 125 eV resolution) and UV-visible absorption spectra (UV/Vis NIR spectrophotometer (JASCO 670) in the wavelength range of 200 to 3200 nm (photon energy of 0.39 eV to 6.2 eV)).



### 3. Results and Discussion

#### 3.1 Structure Analysis

The deposited films were annealed at 400°C for 1h to form crystalline phase for the XRD analysis. Figure 1 illustrates the XRD patterns of the annealed undoped and Cu-doped TiO<sub>2</sub> nanoparticles based thin films. The patterns clearly show peaks of rutile TiO<sub>2</sub> for the prepared TiO<sub>2</sub> and all Cu-doped TiO<sub>2</sub> thin films, the lattice planes of rutile phase (110), (101), (111), (211) at 2θ values 27.4°, 36°, 41.1°, 54.3°. For different contents of Cu-doped samples, no Cu, Cu<sub>2</sub>O or CuO were observed. The formation of rutile phase could be due to higher concentration of the excited clusters producing from the high electron temperature in the plasma, or due to higher energy of the particles impinging on the growing film surface [4].

#### 3.2 Surface morphology, chemical composition, elemental analysis and size distribution

SEM analysis has been conducted to observe the morphology of sample with different contents of Cu-TiO<sub>2</sub>. As seen in Figure 2, the shape of nanoparticles is almost spherical and the thin films are porous with some agglomeration.

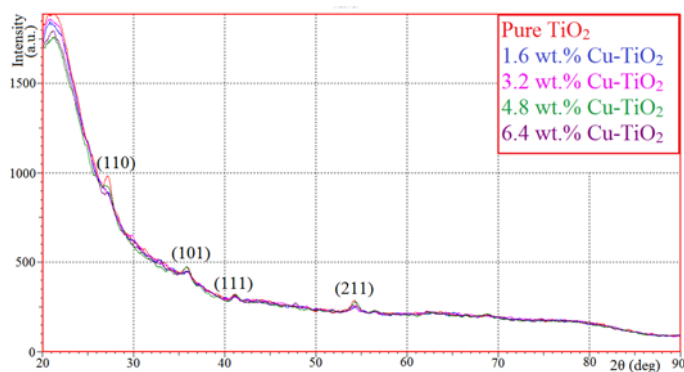


**Figure 1.** XRD patterns of pure TiO<sub>2</sub>, 1.6 wt.% Cu-TiO<sub>2</sub>, 3.2 wt.% Cu-TiO<sub>2</sub>, 4.8 wt.% Cu-TiO<sub>2</sub>, and 6.4 wt.% Cu-TiO<sub>2</sub>.

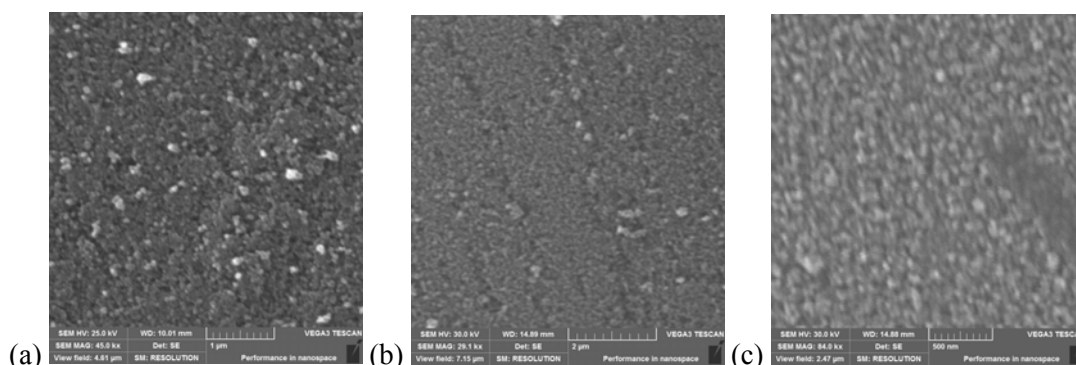


**Figure 2.** SEM images (a) pure TiO<sub>2</sub>, (b) 3.2 wt.% Cu-TiO<sub>2</sub>, and (c) 6.4 wt.% Cu-TiO<sub>2</sub>.

On the other hand, Figure 3 illustrates the EDS analysis for 8% Cu-TiO<sub>2</sub> samples. For thin film Cu, Ti, O, C and Si were detected. Si shows the highest peak which is referred to the substrate (quartz glass). The appearance of C peak is due to the stub used. Both Si and C peaks were ignored in analysis. However, the presence of O reveals that the samples are completely oxidized as soon as they are exposed to air (at room temperature). Thin films have very strong cohesive and adhesive strength, so they can't be wiped out. This makes the prepared films very useful in photocatalytic applications which they can be used repeatedly for several times compared to the coated samples in the sol-gel method, which can be used only once. The small amount of Cu detected could be due to the low concentration in the sample.

Size distribution of Ti-Cu nanoclusters with different Cu contents (1.6, 3.2, 4.8, 6.4, and 8) wt.% measured using the QMF is shown in figure 4. The nanoclusters have a size distribution within the range of 5.4 to 7.1 nm. The intensity of the size distributions at various Cu contents is very low due to the small production yield of nanoclusters. The parameters that have great influence on nanocluster size are the Ar flow,  $f_{Ar}$ , and the aggregation length,  $L$ . In a previous work on pure Ti [5], we found that the changes in the Ar flow and aggregation length affect the nanocluster size and yield. Furthermore, the collision probability plays an important role in controlling the clusters nucleation and growth. The collision probability is detected by the pressure inside the aggregation chamber and by the clusters' residence time inside the cluster source, as reported elsewhere [6]. Therefore, Ar flow rate increases, the clusters will be removed faster, so their residence time in the aggregation chamber will be reduced. Thus when the interaction between the Ar and the clusters and metal atoms is reduced, it enhances a decrease in the clusters size [5]. Moreover, the amount of clusters and aggregates increase with increasing of the deposition time of the Cu-Ti target alloy.

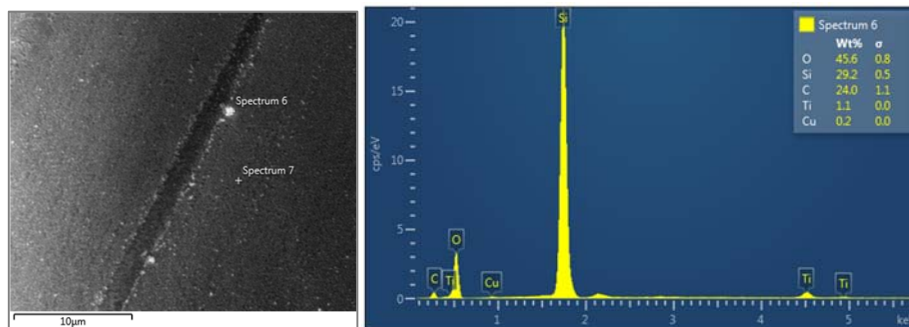


**Figure 3.** EDS analyses for 8 wt.% Cu-TiO<sub>2</sub>.

### 3.3 Optical analysis

Figure 5 shows the UV-Vis absorption spectra of Cu-TiO<sub>2</sub> nanoparticles based thin films of various Cu contents (wt.%). Pure TiO<sub>2</sub> reveals absorption at 389 nm which lies in the range of UV region. Introducing Cu dopant with (1.6, 3.2, 4.8, 6.0, and 8.0 wt.%) resulted in shifting the absorption to the visible region. Absorption spectrum shifts up to 485 nm for the 8wt.% Cu content, which indicates the improvement of the optical activity of Cu-TiO<sub>2</sub> nanoparticles based thin films. The calculated band gap energy for pure TiO<sub>2</sub> and various Cu contents in Cu-TiO<sub>2</sub> thin films are presented in table 1. The band gap energy varies between 3.19 eV (0.0 wt.% Cu or pureTiO<sub>2</sub>) and 2.56 eV (8.0 wt.% Cu). The presence of acceptor states in the band gap could be reason of this change [7]. In addition, transition metals narrow the electronic properties and alter the optical responses of TiO<sub>2</sub>, causing a decrease in the bandgap energy and resulting in wide range absorber of visible light, which can be used in photocatalytic applications.

**Table 1.** Wavelength and band-gap of Cu-doped TiO<sub>2</sub> with various Cu contents.

Cu-TiO <sub>2</sub> (wt.%)	Wavelength (nm)	Band gap (eV)
0.0	389	3.19
1.6	400	3.10
3.2	415	2.99
4.8	431	2.88
6.4	460	2.70
8.0	485	2.56

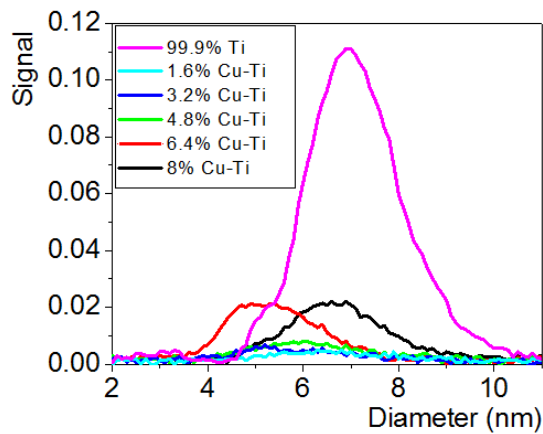


**Figure 4.** Size distribution of Ti-Cu nanoclusters with different Cu contents produced using  $I = 200$  mA,  $f_{Ar} = 35$  sccm,  $L = 90$  mm and  $U/V = 0.12$ .

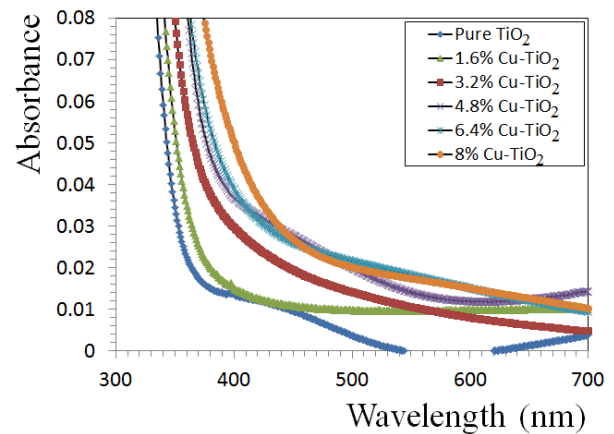


**Figure 5.** UV-Vis absorption spectra of Cu-TiO<sub>2</sub> thin films at various Cu contents (wt.%).

#### 4. Conclusion

The IGC technique was used in this work to prepare thin films of Cu-TiO<sub>2</sub> nanoparticles with various Cu contents (0, 1.6, 3.2, 4.8, 6.0, and 8.0 wt.%). XRD analysis showed a rutile phase of TiO<sub>2</sub>. SEM analysis showed homogeneous nanocluster films with almost spherical nanoclusters. EDS analysis insured the presence of Ti, O and Cu in the Cu-TiO<sub>2</sub> thin film samples. UV-Visible absorption spectra indicated that the presence of Cu in the Cu-TiO<sub>2</sub> thin film samples had shifted the light absorbance to the visible region. Increasing Cu content decreased the band gap energy from 3.19 eV to 2.56 eV. The Cu-doped TiO<sub>2</sub> thin films produced by sputtering are expected to have high activities when used in photocatalytic applications.

#### Acknowledgments

Funded by UAE University (Project #: 31N093) and Emirates Foundation– Grant #: 2011/177 (UAE).

#### References

- [1] Raffi M, Mehrwan S, Bhatti T M, Akhter J I, Hameed A, Yawar W and Ul Hasan M M 2010 *Ann Microbiol* **60** 75–80.
- [2] Guillou N, Nistor L C, Fuess H and Hahn H 1997 *Nanostruct. Mater.* **8** 545-57.
- [3] Mattox D M 2010 Atomistic film growth and some growth-related film properties *Handbook of Physical Vapor Deposition (PVD) Processing* (Elsevier Inc.) 333-98.
- [4] Yamagishi M, Kuriki S, Song P K and Yuzo Shigesato Y 2003 *Thin Solid Films* **442** 227–31.
- [5] Ayesh A I, Ahmed H A, Awwad F, Abu-Eishah S I and Mahmood S T 2013 *J. Mater. Res.* **28** 2622-28.
- [6] Manninen N K, Figueiredo N M, Carvalho S and Cavaleiro A 2014 *Plasma Process. Polym* **11** 629–38.
- [7] Liu B, Zhao X, Zhao Q, He X and Feng J 2005 *J. Electron Spectroscopy & Related Phenomena* **148** 158–63.